Essential role of membrane cholesterol in accelerated BCR internalization and uncoupling from NF-κB in B cell clonal anergy

Mathieu Bléry, Lina Tze, Lisa A. Miosge, Jesse E. Jun, and Christopher C. Goodnow

John Curtin School of Medical Research, The Australian National University, Canberra ACT 2601, Australia

Divergent hypotheses exist to explain how signaling by the B cell receptor (BCR) is initiated after antigen binding and how it is qualitatively altered in anergic B cells to selectively uncouple from nuclear factor κB and c-Jun N-terminal kinase pathways while continuing to activate extracellular signal–regulated kinase and calcium–nuclear factor of activated T cell pathways. Here we find that BCRs on anergic cells are endocytosed at a very enhanced rate upon binding antigen, resulting in a large steady-state pool of intracellularly sequestered receptors that appear to be continuously cycling between surface and intracellular compartments. This endocytic mechanism is exquisitely sensitive to the lowering of plasma membrane cholesterol by methyl-β-cyclodextrin, and, when blocked in this way, the sequestered BCRs return to the cell surface and RelA nuclear accumulation is stimulated. In contrast, when plasma membrane cholesterol is lowered and GM1 sphingolipid markers of membrane rafts are depleted in naive B cells, this does not diminish BCR signaling to calcium or RelA. These results provide a possible explanation for the signaling changes in clonal anergy and indicate that a chief function of membrane cholesterol in B cells is not to initiate BCR signaling, but instead to terminate a subset of signals by rapid receptor internalization.

CORRESPONDENCE
Christopher C. Goodnow:
Chris.Goodnow@anu.edu.au

Abbreviations used: BCR, B cell receptor; ERK, extracellular signal–regulated kinase; HEL, hen egg lysozyme; ITAM, immunoreceptor tyrosine-based activation motif; JNK, c-Jun N-terminal kinase; MBCD, methyl-β-cyclodextrin; PKC, protein kinase C.

A central paradox in the cell biology of the immune system revolves around understanding how the same receptor for antigen can either signal immunogenically to stimulate proliferation and differentiation in response to foreign antigens, or signal tolerogenically to inactivate or eliminate cells that bind to self-antigens. A clear example of this paradox is the phenomenon of clonal anergy in B lymphocytes. Anergy is an active process of immunological self-tolerance brought about by exposure to self-antigens by which self-reactive lymphocytes adopt a state where they are refractory to making an immune response to antigen. Instead, anergic B cells make tolerance-promoting responses to antigen, such as exclusion from lymphoid follicles, apoptosis, or active inhibition of plasma cell differentiation. Corresponding biochemical changes in B cell receptor (BCR) signaling in anergic cells have been identified by analyzing hen egg lysozyme (HEL)-specific B cells that have become anergic to HEL by maturing in animals expressing HEL systemically and comparing them with developmentally matched B cells bearing the same receptor that are naive. In anergic cells, BCR signaling in response to antigen is uncoupled from NF-κB and c-Jun N-terminal kinase (JNK) but continues to activate extracellular signal–regulated kinase (ERK) and calcium oscillations that drive NFAT nuclear shuttling (1, 2). These changes in signaling have major transcriptional and functional consequences (3). The lack of NF-κB activation prevents induction of NF-κB target genes, such as c-myc, IRF4, bcl-XL, and A1 that are normally required for B cell proliferative responses to antigen. The continued activation of NFAT is likely to induce CD5 and CD72, which have inhibitory roles, and the chronic activation of ERK inhibits plasma cell differentiation (4). Similar changes in BCR signaling have been documented in anergic B cells from several transgenic models (5, 6).

The online version of this article contains supplemental material.

The Journal of Experimental Medicine

A key question is how BCR signaling is qualitatively altered in anergic B cells. In naive but not anergic cells, antigen causes IgM and IgD BCRs to partition into a biochemical cell fraction that is relatively resistant to detergent extraction and associated with the cytoskeleton. This occurs before BCR phosphorylation and is unaffected by inhibition of BCR phosphorylation and src kinase activity (7). These results lead to the hypothesis that anergy stems from changes in the subcellular partitioning or trafficking of BCRs. An alternative hypothesis is favored by work in cell lines showing that Igα and Igβ dissociate from membrane IgM and IgD after antigen stimulation and BCR desensitization (8). Moreover, when chimeric BCRs that do not associate with Igα and Igβ are coexpressed with normal BCRs, a minority of these unsheathed BCRs interfere with signaling to antigen in a way that resembles anergy (9).

Resolving how BCR signaling is altered in anergic B cells is made more difficult because of fundamental questions about the basic mechanism of BCR signal transduction. The BCR is formed by a 1:1 protein complex composed of a membrane-bound Ig molecule and a noncovalently associated Igα-Igβ heterodimer (10). The membrane-bound Ig is responsible for the recognition and binding to the antigen, whereas the Igα and Igβ molecules are responsible for signaling to SH2-bearing tyrosine kinases through their immunoreceptor tyrosine-based activation motifs (ITAMs). Several models currently exist to explain how binding of antigen initiates intracellular signal cascades in B cells. In one model, antigen binding causes receptor clustering that in some way favors partitioning of the receptor into cholesterol/sphingolipid-rich membrane microdomains and/or coalescence of these domains. Microdomains are hypothesized to form platforms concentrating important signaling molecules, such as lyn, BTK, and PLCγ2, and excluding inhibitory signaling molecules, such as CD45, to produce an optimal environment around the receptor for initiating signaling (11–13). Alternatively, clustering of antigen receptors may promote tyrosine kinase activation by transphosphorylation independently of the membrane microenvironment (14). Finally, a very different model for initiating BCR signaling (10) proposes that BCR clustering or perturbation by antigen activates syk kinase by BCR-produced H_20_2 and local oxidative inhibition of tyrosine phosphatases (15). In the latter models, association of BCRs with cholesterol-rich microdomains plays no role in signal initiation but might favor interactions with microdomain-associated Lyn kinase to terminate signaling, consistent with Lyn's critical in vivo role as a BCR signal inhibitor (16, 17). Thus, there are widely divergent views on the mechanism of BCR signal initiation and the role of membrane microdomains.

To understand how the BCR is selectively uncoupled from NF-κB in anergic cells, in this study we have compared the fate of cell surface receptors in naive and anergic B cells and the effects of depleting membrane cholesterol. We identify a striking alteration in BCR subcellular partitioning, involving a dramatically enhanced shuttling and temporary sequestration of BCRs intracellularly. Paradoxically, given the view that cholesterol-rich microdomains promote BCR signaling, we find that decreasing membrane cholesterol does not disrupt immunogenic signaling to calcium or NF-κB in naive B cells, but completely inhibits and reverses BCR sequestration in anergic cells resulting in reactivation of signals to NF-κB. These results indicate that membrane cholesterol serves a chief, rate-limiting role to inhibit signaling by BCRs, at least in part through promoting a process of receptor endocytosis and recycling that is remarkably enhanced in anergic cells.

RESULTS

Monomeric HEL does not induce capping of surface IgD despite being a potent inducer of RelA nuclear accumulation in naive B lymphocytes

Previous data demonstrated that anergic B cells have a similar amount of surface IgD to naive controls (18) and that there is no detectable difference between IgM and IgD in their capacity to activate naive HEL-specific cells (19). In addition, our previous biochemical data from fractionated cell extracts indicated differences in IgM and IgD association with membrane/cytoskeletal fractions in anergic cells (7). We used confocal microscopy to investigate the possibility that uncoupling from NF-κB was associated with differences in subcellular distribution of the BCR on the cell membrane. IgD localization and activation of the NF-κB pathway were followed in the same cells using confocal microscopy after staining permeabilized cells with antibodies to IgD and the NF-κB subunit RelA.

On naive B cells (BCR Tg cells), IgD staining with or without permeabilization of the membrane with Triton X-100 was comparable, indicating that most of the IgD is on the cell surface and diffusely distributed before stimulation (Fig. 1, B and D). Stimulation with monomeric HEL did not induce any appreciable patching or capping of the surface IgD but nevertheless efficiently induced accumulation of RelA in the nucleus of the naive B cells (Fig. 1, A and F, and Figs. S2 and S3, which are available at http://www.jem.org/cgi/content/full/jem.20060552/DC1). These results indicate that microscopically visible patching or capping of receptors is not required for efficient signaling. Interestingly, parallel studies using stimulation of the BCR on naive B cells with a nonmitogenic preparation of goat anti-κ light chain antibody induced very large caps of IgD but without appreciable accumulation of RelA in the nucleus (Fig. 1, A, C, and E). Collectively, these data emphasize the weak correlation between BCR capping and immunogenic signaling to the NF-κB signaling pathway and indicate that if raft-coalescing mechanisms are involved in this signaling, they must occur at a submicron scale not readily resolvable by the light microscope.

Anergic B cells have an intracellular sequestered pool of IgD

In opposition to naive B cells, the staining pattern of IgD in permeabilized versus nonpermeabilized anergic cells

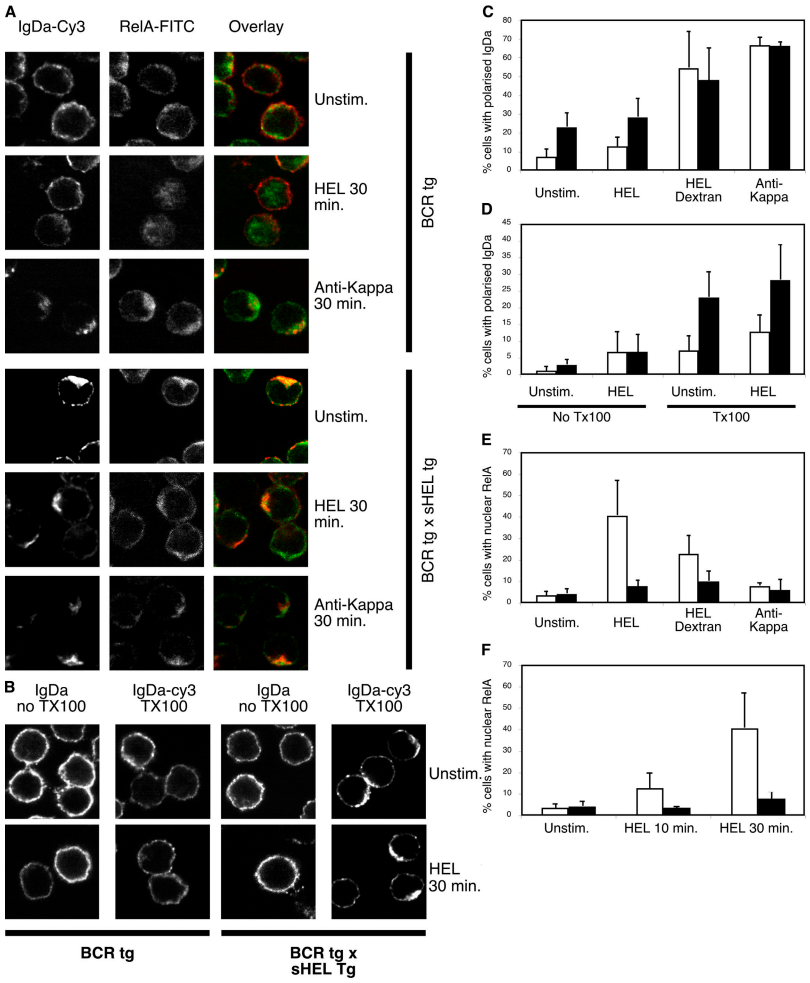

Figure 1. Anergic B cells fail to accumulate RelA in the nucleus but contain a large pool of intracellular IgD. (A) Immunofluorescent staining and confocal observations were performed on Triton X-100–permeabilized naive B cells (BCR tg) or anergic B cells (BCR tg x sHEL tg). Staining for IgD^a and RelA was analyzed after HEL stimulation (HEL 30 min), goat anti-κ light chain stimulation (Anti-Kappa 30 min), or without stimulation (Unstim.). Note that the thin rim of cytoplasmic and plasma membrane staining for IgD readily demarcates the nucleus of these small lymphocytes. (B) IgD staining was performed on Triton X-100–permeabilized or on nonpermeabilized (no TX100) cells to compare the distribution of surface receptors only with the distribution of intracellular plus surface IgD receptors. (C) 300–900 permeabilized cells were observed per condition per experiment, and cells displaying a polarized accumulation of IgD^a at one pole in the focal plane were counted. Mean + SD values are obtained from three to six independent experiments. (D) As in C, except that cells were either not permeabilized (no TX100) or permeabilized (TX100) before staining for IgD. (E and F) As C and D, cells displaying predominantly nuclear localization of RelA in the midline focal plane of the cells, as shown in A, were counted. Open bars, BCR tg; filled bars, BCR tg x sHEL tg. Stimulation time is 30 min for C, D, and E and as indicated in F.

(BCR tg x sHEL tg cells) revealed striking differences. In nonpermeabilized cells, cell surface IgD was distributed homogeneously around the plasma membrane (Fig. 1 B, no TX100). Once permeabilized, however, anergic cells uniquely exhibited a large pool of IgD polarized at one pole of the cell, apparently under the plasma membrane in the confocal plane of observation (Fig. 1, B and D, and Figs. S2 and S3). To confirm this observation, the cells were stained first with anti–IgD^a-FITC to reveal and saturate cell surface receptors, and the cells were then fixed, permeabilized, and restained with IgD^a-Cy3 to reveal intracellular IgD. The results confirmed the existence of a large intracellular pool of IgD in anergic cells (Fig. 2 A and Fig. S4, which is available at http://www.jem.org/cgi/content/full/jem.20060552/DC1). In addition, cells were incubated with HEL-biotin at 4°C, fixed, saponin permeabilized, and stained with SAV-PE and an anti-HEL mAb coupled to cychrome (Fig. S5, available at http://www.jem.org/cgi/content/full/jem.20060552/DC1). FACS plots are shown in Fig. 2 B and demonstrate the presence of a large pool of antigen inside anergic cells correlating with the existence of an intracellular pool of IgD in these cells. As previously described using biochemical methods, HEL stimulation did not stimulate nuclear accumulation of RelA in anergic B cells (Fig. 1, A, E, and F, and Fig. S3) (2).

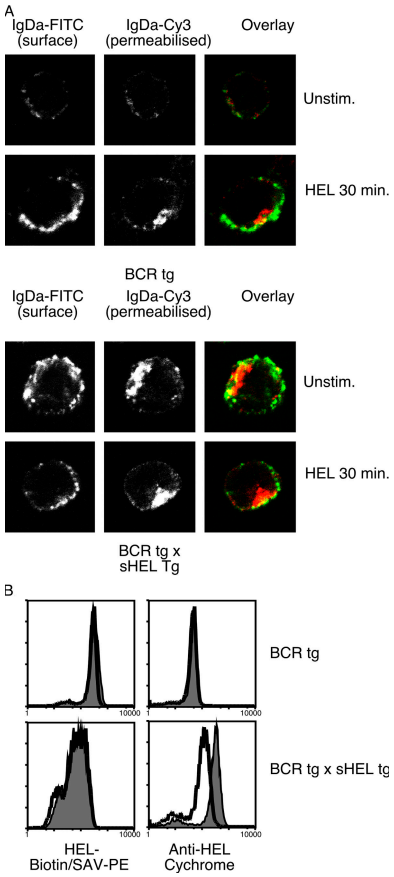

Figure 2. Polarized intracellular accumulation of IgD and antigen in anergic B cells. (A) Representative confocal images of naive or anergic B cells. Cells were stimulated as indicated, placed on ice, stained with saturating doses of an anti–IgD^a-FITC mAb (IgD^a-FITC, surface), and then fixed, permeabilized, and stained with an anti-IgD^a mAb-biotin and SAV-Cy3 (IgD^a-Cy3, permeabilized) to reveal intracellular IgD. (B) FACS staining on unstimulated naive or anergic cells, either nonpermeabilized (bold lines) or saponin permeabilized (shaded histograms). Surface BCRs available to bind HEL were measured by staining with HEL-biotin before saponin treatment, followed by streptavidin-PE, whereas all BCR-bound HEL antigen was stained with anti–HEL cychrome antibody. Note that the anti-HEL cychrome staining of anergic cells is twice as high on permeabilized cells compared with nonpermeabilized cells, demonstrating that half of the HEL-engaged BCRs are located intracellularly. There is no difference in surface IgD staining between the naive and anergic cells, and the lower staining for HEL-biotin on the latter reflects occupancy of half of the surface BCRs with untagged HEL and down-regulation of surface IgM.

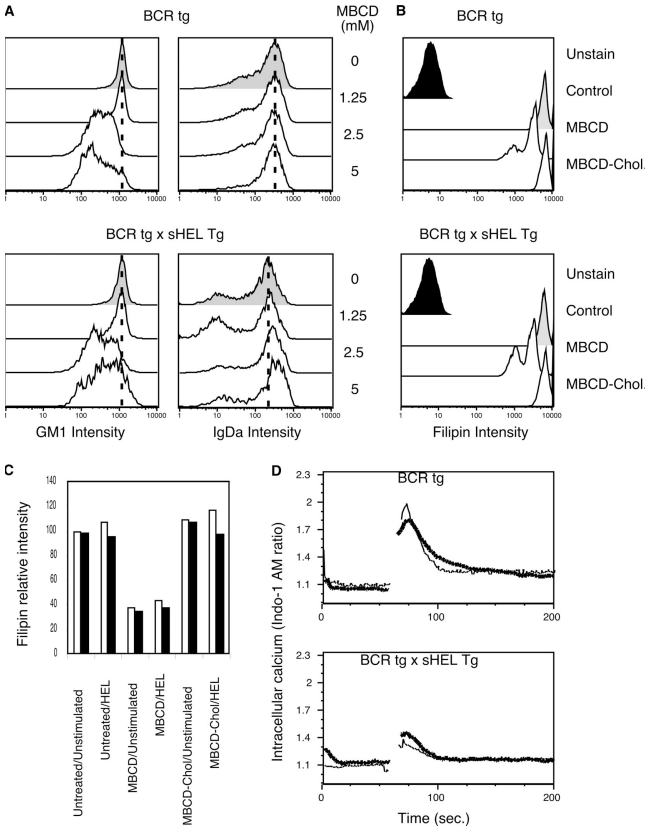

Figure 3. Effects of depleting cholesterol from membranes of naive and anergic B cells. (A) Surface levels of raft-associated GM1 sphingolipids and IgD^a were measured by flow cytometry before (gray histogram) and after treatment with the indicated concentrations of MBCD (open histograms). The dotted lines serve as an arbitrary visual reference for control fluorescence levels. (B) Membrane cholesterol levels were measured by staining with filipin and flow cytometric measurement of filipin fluorescence on untreated cells (Control), MBCD-treated cells (MBCD), or cells treated with MBCD that had been preloaded with cholesterol (MBCD-Chol). (C) Values of the mean fluorescence of the filipin staining were normalized with the value obtained for untreated and unstimulated BCR tg cells. Open bars, BCR tg cells; filled bars, BCR tg x HEL tg cells. Data shown are representative of two to five independent experiments. (D) HEL antigen-induced calcium responses were recorded as variations in the Indo-1 fluorescence ratio gated on the B220$^+$ cell population. Bold lines, calcium response of control cells; thin lines, cells that were first pretreated with 2.5 mM MBCD. Stimulation is performed after 60 s with soluble HEL. Experiment shown is representative of five independent experiments.

Membrane cholesterol extraction does not interfere with BCR signaling to antigen in naive cells

The next experiments were designed to investigate whether or not cholesterol-rich microdomains were involved in the differences in NF-κB signaling by BCRs on naive and anergic cells. The small cyclic oligosaccharide methyl-β-cyclodextrin (MBCD) binds cholesterol reversibly, allowing cholesterol to be depleted from or added to cell membranes (20). To measure the lowering of plasma membrane cholesterol by MBCD, cells were stained for FACS with the antibiotic filipin, which binds to cholesterol and has fluorescent properties (21). Filipin staining decreased ~50% upon MBCD treatment (Fig. 3, B and C). Treatment with cholesterol-loaded MBCD did not significantly change the level of filipin staining from mock-treated controls (Fig. 3, B and C) and was therefore used as an additional control to exclude possible nonspecific effects of MBCD. Cholesterol depletion by MBCD was reversible by subsequent treatment with MBCD loaded with cholesterol (not depicted). In addition to lowering plasma membrane cholesterol, MBCD treatment also

dramatically reduced the amount of cell surface GM1 glycosphingolipids, as measured by staining with fluorescent cholera toxin B subunit (Fig. 3 A). This result is consistent with disruption of lipid rafts by cholesterol lowering with MBCD. Despite the clear effects of MBCD on the plasma membrane composition of naive B cells, this procedure had no effect on the expression of surface IgD (Fig. 3 A) and, surprisingly, did not interfere with antigen-induced calcium responses (Fig. 3 D) or RelA nuclear translocation (Fig. 4, A and B).

Cholesterol depletion redistributes sequestered IgD to the cell surface and restores RelA nuclear accumulation in anergic cells

The effects of MBCD treatment were studied in parallel in anergic B cells. There were no differences in filipin staining between untreated naive and anergic B cells, indicating that the levels of free cholesterol in the membrane are comparable (Fig. 3, B and C). Likewise, there was no difference between anergic and naive B cells in plasma membrane GM1 glycosphingolipids stained with cholera toxin (Fig. 3 A). MBCD treatment diminished filipin and cholera toxin staining to a comparable amount on anergic B cells and had no effect on antigen-induced calcium responses (Fig. 3, A, C, and D). However, in contrast to naive B cells, when anergic B cells were treated with MBCD there was a striking effect on cell surface IgD expression, with the median amount of surface IgD increasing ~50% (Fig. 3 A). In parallel, confocal microscopy showed that the intracellular pool of IgD was diminished (Fig. 4 C). Thus, the intracellular pool of sequestered IgD in anergic cells is maintained by a cholesterol-dependent mechanism and is redistributed to the cell surface when cholesterol is lowered.

Surprisingly, MBCD treatment of anergic cells also induced accumulation of RelA in the nucleus (Fig. 4, A and B). This effect appeared spontaneous in that it did not require HEL antigen to be added to the anergic cells in vitro and was not augmented by adding antigen to the cells in vitro. However, the RelA translocation is likely to be antigen dependent because more than half of the antigen receptors on anergic cells are already occupied with HEL antigen in vivo, and no RelA translocation was stimulated by MBCD in naive cells lacking HEL on their receptors. Thus, the lowering of membrane cholesterol by MBCD in anergic cells appears to reestablish BCR signaling to NF-κB.

Accelerated BCR endocytosis in anergic B cells and its disruption by plasma membrane cholesterol extraction

The data described above demonstrated that the intracellular pool of sequestered IgD in anergic cells required membrane

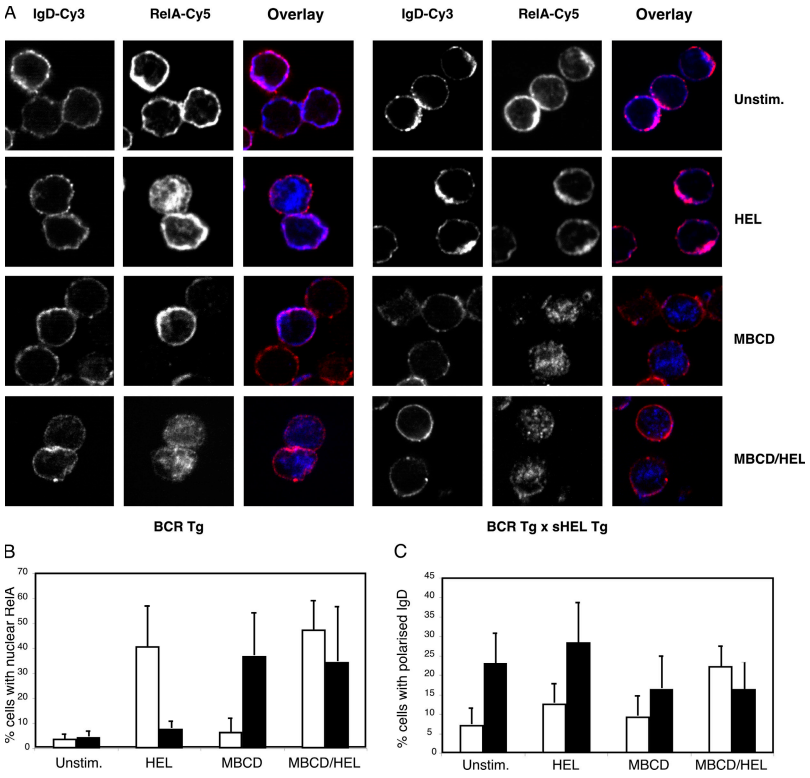

Figure 4. MBCD treatment restores RelA nuclear accumulation in anergic B lymphocytes. (A) Staining for IgD^a and RelA and confocal analysis were performed on permeabilized B cells. The cells were first treated with MBCD or left untreated, and then either stimulated with HEL for 30 min or left unstimulated, as indicated. (B) Quantitation of cells with nuclear RelA accumulation. Open bars, naive BCR tg cells; filled bars, anergic BCR tg x HEL tg cells. Mean + SD is calculated from three independent experiments, where 300–900 cells were counted each time. (C) As in B, but cells with polarized IgD^a staining were counted.

cholesterol to be maintained (Fig. 3 A), but this gave no information about the dynamics of this pool and whether cholesterol was required to promote IgD removal from the cell surface or prevent recycling back to the cell surface. A flow cytometric method was developed to measure the rate of endocytosis of antigen receptors. Cells were incubated on ice with HEL antigen coupled covalently to PE (HEL-PE), and then the cells were placed at 37 or 4°C for varying periods of time. Endocytosis can only occur at 37°C and was stopped at different times by placing the cells on ice. The cells were then exposed to a brief acid wash, which rapidly inactivates the fluorescence of phycoerythrin remaining on the cell surface. Endocytosed HEL-PE is protected from acid exposure inside the cell and remains brightly fluorescent, allowing sensitive measurement of the proportion of initially bound antigen that has been internalized (Fig. 5 A). Endocytosis of the antigen occurred rapidly within the first minute at 37°C in anergic B cells, and most of the bound fluorescent antigen is protected within 10 min (Fig. 5 B). In contrast, endocytosis in naive cells had a slower onset, and the fraction of bound fluorescent antigen that was protected was half that achieved in anergic cells (Fig. 5 B). Quantifying the rate of endocytosis over the first 10 min using the method of Liu et al. (22) demonstrated an approximate doubling in anergic cells compared with their naive counterparts (Fig. 5 B, right).

Depletion of plasma membrane cholesterol with MBCD dramatically inhibited the rate and overall amount of antigen endocytosis in both anergic and naive B cells (Fig. 5 B). Endocytosis of antigen was also inhibited by a specific inhibitor of Src kinase activity, PP1, and by an actin polymerisation inhibitor, latrunculin B (Fig. 5 C). Endocytosis of antigen was inhibited by the protein kinase C (PKC) inhibitor rottlerin. Rottlerin is specific for PKC-δ at low concentration (3–6 μM), inhibits PKC-β and PKC-γ at medium concentration (30–42 μM), and inhibits PKC-ε, PKC-η, and PKC-ζ at high concentration (80–100 μM) (23). Endocytosis of the antigen was 50% inhibited by 5 μM rottlerin (Fig. 5 C). This result suggests that endocytosis is dependent on PKC-δ, although this conclusion must be qualified by the broad potential specificity of this compound. Collectively, these results indicate that a rapid, active, cholesterol-dependent process of BCR endocytosis is dramatically enhanced in anergic cells compared with naive cells. When endocytosis is stopped by MBCD treatment, the receptors recycle and accumulate back on the cell surface.

The rapid rate of internalization is consistent with clathrin-mediated BCR internalization, which has been shown to be the major pathway for BCR endocytosis and depends upon membrane cholesterol and clathrin phosphorylation by lyn kinase (24, 25). Clathrin-mediated endocytosis is blocked by depleting cellular potassium or by the presence of sucrose in the extracellular fluid. In four independent experiments, sucrose decreased HEL-PE endocytosis to 4 ± 3% (mean ± SD) of control levels in naive cells and to 7 ± 8% in anergic cells. Potassium depletion decreased internalization to 37 ± 31% and 40 ± 28% of control levels in naive and anergic cells, respectively. There were no significant differences between naive and anergic cells in the relative inhibition by either agent, indicating that the accelerated rate of endocytosis in anergic cells occurs by the same clathrin-mediated pathway that occurs in naive B cells.

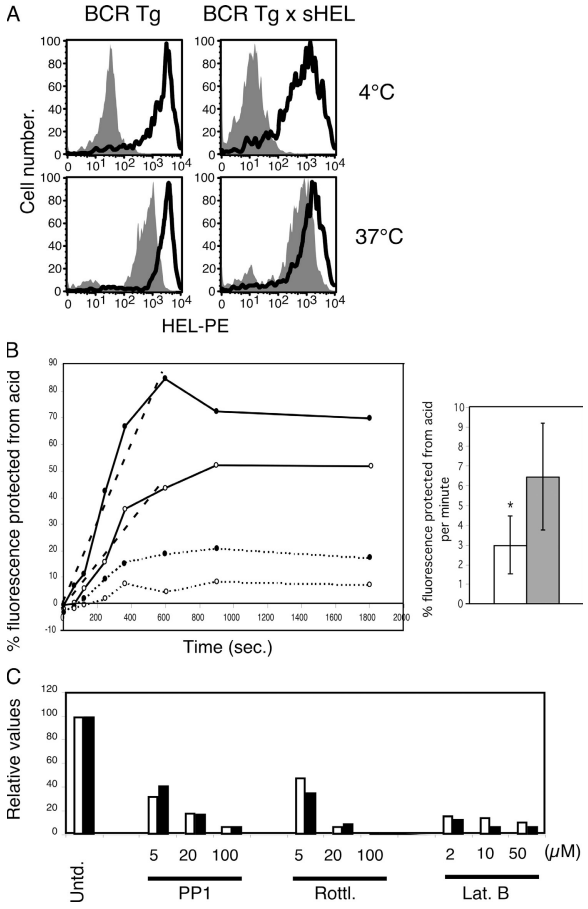

Figure 5. Enhanced BCR endocytosis in anergic cells. (A) Histograms showing HEL-PE fluorescence of B220$^+$ naive (BCR) or anergic (BCR tg x sHEL tg) cells. Cells were either acid treated to inactivate the fluorescence of cell surface PE so remaining signal measures endocytosed antigen (shaded histograms), whereas control cells (open histograms) provide a measure of total surface and intracellular HEL-PE. Cells kept at 4°C serve as a no endocytosis control, whereas cells warmed to 37°C for 10 min before acid treatment reveal the fraction of bound antigen that has been internalized. (B) Time course of antigen endocytosis. ●, anergic B cells; ○, naive B cells. Dashed lines show endocytosis by cells with cholesterol lowered by 2.5 mM MBCD, and solid lines are corresponding values for mock-treated controls. The experiment shown is representative of three independent experiments. The right panel shows the rate of endocytosis for the first 10 min calculated from the dashed line on the left panel. Values represent the mean of three independent experiments. (C) Pharmacological inhibition of antigen endocytosis in naive cells (open columns) and anergic cells (filled columns). The amount of antigen endocytosed by untreated cells after 10 min was set to 100%. The effect of each treatment is expressed as relative endocytosis compared with the untreated value (Untd.). PP1, rottlerin (Rottl.), and latrunculin B (Lat B) were used at the indicated concentrations. Data shown are representative of two to five independent experiments.

To distinguish if the endocytosed antigen receptors on anergic cells normally recycle back to the cell surface or only after MBCD lowering of cholesterol, we developed a FACS assay to measure receptor recycling (Fig. 6). HEL antigen was labeled with biotin coupled via a thiol-cleavable linker. After occupying surface BCRs with HEL-SS-biotin and allowing endocytosis at 37°C for 10 min, antigen remaining on the surface was cleaved from its biotin tag by exposure to MESNA, a membrane-impermeant reducing agent. Thus, intracellularly sequestered antigen would selectively retain biotin label. After cleavage, we cultured the cells at 37°C for varying times to allow internalized antigen to return to the cell surface, where it was detected by staining with streptavidin coupled to allophycocyanin. Using this assay, 14 ± 5% (mean ± SD) of internalized antigen could be shown to return to the cell surface of anergic cells within 3 min, and 10 ± 5% was recycled at the same time in naive cells (Fig. 6, A and B). The fraction of endocytosed receptors recycled back to the surface is likely to be an underestimate because of the rapid rate of internalization (Fig. 5). The higher percentage of initially antigen-labeled receptors coming back to the surface in anergic cells suggested a more rapid shuttling of BCRs between the surface and the intracellular compartment (Fig. 6 B).

DISCUSSION

The data described above provide an unexpected insight into the role of membrane cholesterol in BCR signaling and the mechanisms for altering signaling in anergic B cells. We find that antigen-engaged BCRs on anergic cells are endocytosed at twice the rate of naive cells, resulting in a large steady-state pool of intracellularly sequestered receptors and antigen that appear to be rapidly exchanging between surface and intracellular compartments (Figs. 1, 2, 5, and 6). This endocytic mechanism is exquisitely sensitive to cholesterol lowering by MBCD. When endocytosis is blocked, the intracellular BCRs with antigen bound to them accumulate on the plasma membrane to increase the surface IgD density on anergic cells (Fig. 3) and RelA nuclear accumulation is stimulated when previously it was blocked. Moreover, when plasma membrane cholesterol is lowered and GM1 sphingolipid markers of membrane rafts are greatly reduced in naive B cells, this does not diminish BCR signaling to calcium or RelA.

It is surprising that MBCD treatment of naive cells, despite markedly lowering membrane cholesterol and GM1, does not interfere with initiation of BCR signals for calcium or for RelA translocation. In the simplest terms, this result does not support the hypothesis that initiation of BCR signaling depends on translocation to cholesterol and GM1-rich lipid rafts (13). Membrane cholesterol can only be lowered by ~50% to still maintain good B cell viability; however, it could reasonably be argued that the cholesterol-dependent rafts needed to initiate signaling are either difficult to extract or tolerate a moderate reduction in cholesterol and GM1 content. The data are nevertheless more consistent with the alternative hypotheses that BCR signaling is initiated by cholesterol-independent mechanisms for altering the balance between syk and tyrosine phosphatase activity (14, 15). Also favoring this view are other findings that BCR signaling is initiated outside lipid rafts in the immature B cell line WEHI-231 (26) and the observation in the Ramos cell line that disrupting microdomains by cholesterol lowering with MBCD does not interfere with BCR signaling to calcium but instead enhances it (27). Taken together with our results in anergic cells, this suggests that the critical, rate-limiting function of

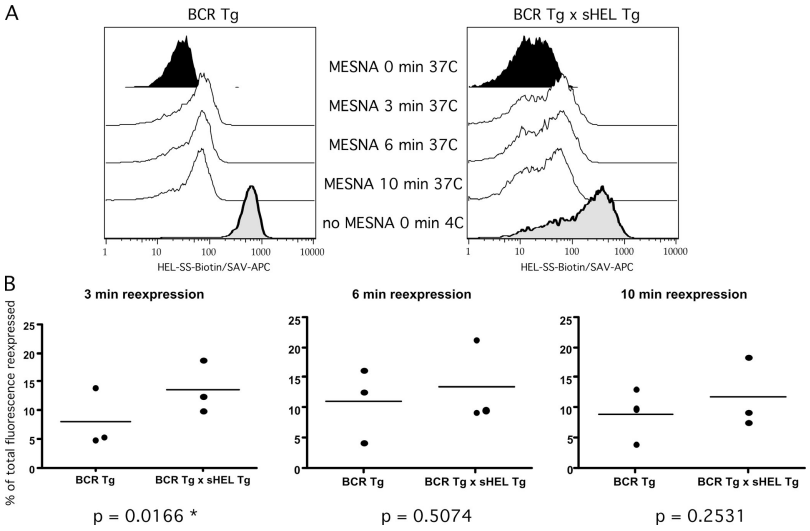

Figure 6. Rapid recycling of antigen-loaded BCRs to the cell surface. (A) Naive or anergic B cells were incubated with HEL-SS-biotin at 4°C, warmed to 37°C for 10 min to allow endocytosis, and then the remaining surface antigen was cleaved of biotin with MESNA. The cells were then warmed again to 37°C for the indicated times and stained with streptavidin-APC to detect material returning to the cell surface. The experiment shown is representative of three independent experiments. (B) Percentage of reexpressed receptor bound to antigen in three independent experiments.

MBCD-sensitive cholesterol in the membrane is to inhibit BCR signaling to RelA by promoting endocytosis.

These data do not exclude a separate role for coalescence of lipid rafts or attachment to the plasma membrane cytoskeleton so that they remain on the cell surface, for example as part of the process of sustaining immunogenic BCR signaling by Btk (28) or enhancing signaling through CD21/CD19 (29, 30). Formation of an endocytosis-resistant cytoskeletally attached microdomain as an early step in immunogenic signaling would be consistent with the observation that BCRs on naive but not anergic cells associate with detergent-resistant domains attached to the cytoskeleton, before and independently of src kinase activation (7). These microdomains may be organized simply by cytoskeletal specializations and not necessarily involve cholesterol-rich membrane domains. Formation of a putative B cell synapse by coalescence of lipid rafts has been proposed to be important to form stable complexes that would eventually be capped and internalized (13). Microscopically visible structures that could correspond to an immunogenic B cell synapse have been documented between HEL-specific splenic B cells and antigen-presenting cells displaying membrane-bound HEL (31). The significance attributed to visible, micron-sized rearrangements must be tempered, however, by functional data showing that the optimal number of receptors that need to be stably collected into a single cluster on the cell surface for an immunogenic B cell response—a so-called immunon—is in the order of 16–20, which represents a structure in the nanometer scale (32, 33). Similarly, HEL antigen signals efficiently to NF-κB without forming microscopically visible patches or caps, whereas extensive capping of BCRs and co-capping of GM1 with an anti-κ antiserum is not accompanied by effective NF-κB signaling (Fig. 1).

Accelerated cycles of IgD endocytosis and reexpression may account for the uncoupling of signals to NF-κB and JNK as well as for the continued signaling to ERK and chronic oscillatory stimulation of calcium that collectively distinguish anergic B cells from naive cells. ERK activation and low calcium oscillations in anergic cells are not constitutive events but require continued reexposure to HEL antigen (1). It is notable that calcium elevation and ERK activation occur within seconds of antigen binding to naive B cells, whereas NF-κB and JNK activation take several minutes. We find that endocytosis begins within 1 min in anergic cells (Fig. 5). A member of the membrane-associated guanylate kinase family of proteins, Carma1 (also called Card-11), is critical for BCR signaling to NF-κB and JNK but not required for calcium, NFAT, or ERK activation (34). Carma1 has numerous protein–protein interaction sites and, by analogy with membrane-associated guanylate kinase proteins at the postsynaptic densities of neurons, is required to assemble an elaborate signaling complex (an "immunosome") at the plasma membrane comprising surface receptors and signaling molecules for NF-κB and JNK activation (34–37). The accelerated endocytosis of BCRs in anergic cells may frustrate assembly of the Carma1 immunosome needed for NF-κB and JNK signaling, and may withdraw the BCR from the plasma membrane pool of PIP2 needed as a substrate for PLCγ, thus limiting intracellular calcium to low oscillations. The sustained BCR signaling to ERK in anergic cells is consistent with recent data from receptor tyrosine kinases and the adrenergic receptor showing that signaling to ERK via src kinases continues after receptor sequestration to recycling endosomes (38). The correlation between inhibition of endocytosis and induction of RelA nuclear accumulation when cholesterol is lowered in anergic cells nevertheless does not establish a direct linkage between these two effects. It is conceivable that a cholesterol-dependent process other than endocytosis is responsible for preventing RelA nuclear accumulation in anergic cells.

Several independent lines of evidence support the conclusion that accelerated BCR endocytosis in anergic cells contributes to their diminished proliferative response. Stoddart et al. (24, 25) have shown that rapid BCR internalization at the rate observed here depends upon clathrin heavy chain and its phosphorylation by tyrosine kinases in cholesterol-dependent membrane domains. When clathrin-mediated endocytosis is blocked in DT40 cells, BCR induced tyrosine phosphorylation and ERK activation is prolonged. The accelerated internalization of BCRs on anergic cells resembles that observed in splenic B cells from $Ig\beta_c->\alpha_c$ gene-targeted mice engineered to bear two copies of the Igα cytoplasmic tail in the BCR instead of a heterodimer of Igα and Igβ tails (39). B cells in $Ig\beta_c->\alpha_c$ mice are also anergic, displaying diminished calcium and proliferative responses to BCR engagement. Comparison with and crosses to mice with mutated Igα ITAM tyrosines demonstrated that the diminished surface IgD density and anergy of $Ig\beta_c->\alpha_c$ B cells is partly corrected by halving the number of functional ITAMs per BCR (39). Collectively, these results indicate that B cell anergy involves augmentation of an inhibitory process of clathrin/cholesterol-dependent endocytosis that depends upon *src* family kinases, BCR ITAM phosphorylation, and unique residues in the Igα cytoplasmic tail.

The observation that BCR endocytosis in anergic and naive cells is inhibited by rottlerin at low concentration suggests that PKC-δ is required (Fig. 5). This observation is interesting in light of data from Mecklenbrauker et al. (40) who showed that PKC-δ was necessary for B cell anergy and preventing RelA nuclear accumulation in the same model analyzed here. PKC-δ may thus favor tolerogenic signaling, in part by promoting endocytosis of the anergic receptor or its localization to MBCD-sensitive domains.

Collectively, our data reveal an acceleration of BCR endocytosis and a surprising relationship between membrane cholesterol, BCR endocytosis, and RelA nuclear accumulation that may explain the qualitative changes in BCR signaling in B cell clonal anergy. It will be important in future work to explore how this mechanism is enhanced in anergy and how it may be regulated in other situations where antigen receptor signals are qualitatively altered, such as B cell memory and T cell anergy.

MATERIALS AND METHODS

Mice. Mice transgenic for the MD4 anti-HEL–specific BCR were bred either to B6 mice (BCR tg) or to mice expressing the soluble HEL ML5 transgene (BCR tg x HEL tg) (41). All mice used were between 11 and 22 wk of age. All experiments involving animals were performed under protocols approved by the Animal Ethics & Experimentation Committee of The Australian National University.

Antibodies and drugs. Biotinylated anti-CD43, biotinylated anti-Ter119, and anti–Igβ-FITC were purchased from BD Biosciences, and rabbit anti-RelA was from Santa Cruz Biotechnology, Inc. The anti-IgDa AMS9.1-biotin and the B220-FITC were produced and purified in our laboratory. HEL conjugated to PE (HEL-PE) was prepared by reductive cross-linking of R-PE with HEL. In brief, 11 μl of 10 mg/ml SMCC (succinimidyl 4-(*N*-maleimidomethyl)cyclohexane-1-carboxylate; Pierce Chemical Co.) in DMSO per mg of R-PE in 50 mM sodium phosphate, pH 7.01, 1 mM EDTA was incubated for 60 min at room temperature to yield a maleimide-labeled PE. HEL was reduced in 50 mM MES buffer with 20 mM DTT. Excess reagents were removed, and buffer pH was changed by passing both preparations on D-salt excellulose desalting column (Pierce Chemical Co.) to have both preparations in 50 mM MES, pH 6.0, 2 mM EDTA. Coupling consisted of reacting maleimide groups on the PE with free sulfhydryl groups on the HEL molecules. 3.2 mg PE per mg of HEL was incubated at room temperature for 50 min and 34 μg *N*-ethyl maleimide at 100 mg/ml in DMSO was added per mg of HEL for 20 min at room temperature to stop the reaction. Conjugated HEL-PE was finally dialyzed in PBS. Streptavidin (SAV)-Cy3 and donkey anti–rabbit IgG-Cy5 or FITC were obtained from Jackson ImmunoResearch Laboratories. MBCD, filipin, nystatin, sucrose, HEL, and latrunculin B were obtained from Sigma-Aldrich. Rottlerin was from Pierce Chemical Co. and was provided by N. Ozsarac (John Curtin School of Medical Research [JCSMR], Canberra City, Australia). HEL-dextran was provided by C. Garcia de Vinuesa (JCSMR). Indo-1-AM was purchased from Invitrogen and used at 1 μM according to the manufacturer's instructions. Calcium analysis was acquired on an LSR flow cytometer (Becton Dickinson) and analyzed with FlowJo (Tree Star Inc.).

B cell purification and stimulation. Splenocytes from mice were subjected to a negative selection using biotinylated anti-CD43 and anti-Ter119 antibodies with magnetic MACS beads coupled to streptavidin (Miltenyi Biotec) in DMEM without phenol red 2% FCS, 10 mM Hepes, 0.1 mM nonessential amino acids, 1 mM sodium pyruvate, and 55 μM 2-ME and supplemented with penicillin and streptomycin (referred hereafter as "medium") as described previously (7). 90–98% $B220^+$ cell purity was routinely achieved. Pretreatment of the cells at 2×10^7 cells per ml with drugs was performed in microcentrifuge tubes in medium for 30 min at 37°C as indicated in the figures. For filipin, nystatin, and hypertonic sucrose treatment, there was no serum in the medium. Concentrated soluble HEL was then added to a final concentration of 10 μg/ml for the time indicated. A dose response to MBCD established that concentrations higher than 5 mM caused B cell death, but those at 2.5–5 mM caused little cell death. Untreated cells were also preincubated for 30 min at 37°C before stimulation. 2.5 mM MBCD loaded with cholesterol was prepared as described by Christian et al. (20). Potassium depletion treatment was performed by incubating the cells for 5 min at 37°C in a 1:1 mix of medium and distilled water. Cells were then put in water containing 100 mM NaCl and 50 mM Hepes for 20 min before stimulation. The cells were kept in that buffer for all subsequent steps.

Confocal microscopy. After stimulation, ice-cold PBS was used to wash the cells and cells were allowed to rest on 0.1% poly-L-lysine–coated coverslips for 5 min before a 2-min spin at 94 *g*. Fixation was performed for 10 min at 4°C followed by 10 min at room temperature with 2% paraformaldehyde (PFA) in PBS. Quenching of the PFA was done for 15 min with 0.1% NaBH4 in PBS, and cells were permeabilized (if indicated) with 0.1% Triton X-100 in PBS for 4 min. Blocking was performed for 30 min in PBS containing 0.1% gelatin, 5% BSA, 2% serum from the species of the secondary antibody used, 0.1% azide, and 1 μg/ml Fc block (anti-CD16/32 from BD Biosciences). All of these steps were performed at room temperature. Antibodies were incubated from 1 h at room temperature to overnight at 4°C in PBS containing 0.1% BSA and 0.1% azide, coverslips were washed, and fluorescent secondary antibodies were incubated for 1 h at room temperature. Several washes in PBS and in water were performed before mounting coverslips onto slides with fluorescent mounting medium (DakoCytomation). Observations were performed with a Radiance 2000 confocal microscope using Laser Sharp software (Bio-Rad Laboratories). Sequential acquisitions of each channel were performed to avoid compensation problems. Single color controls and secondary antibody controls were used to set up the detectors. A z-stack of confocal sections was collected, and sections through the midline of the cell nucleus were used for analysis as illustrated in Fig. S1, which is available at http://www.jem.org/cgi/content/full/jem.20060552/DC1. Images were processed and analyzed using Graphic Converter and Adobe Photoshop software.

Endocytosis assay. 4×10^6 splenocytes at 2×10^7 cells per ml were incubated in DMEM medium as described above, with 10 μg/ml HEL-PE in microcentrifuge tubes on ice for 30 min. Cells were washed once with medium and resuspended in medium at 2×10^7 cells per ml, and the suspension was split in equal proportions in two new tubes and incubated at 4 or 37°C for the time indicated. Each cell suspension was again split between two new tubes on ice. One tube was centrifuged at 500 *g*, and the cells were resuspended at 2×10^7 cells per ml in PBS 0.1% BSA, 0.1% azide for FACS staining and held on ice (untreated samples). In the second tube, cells were centrifuged at 500 *g* and resuspended in 0.5 ml of 150 mM NaCl, 150 mM acetic acid, pH 2.7, and left on ice for 3 min before the addition of 0.5 ml FCS (FCS was added directly to the tube to stop the acid treatment). After centrifugation and removal of supernatant, this treatment was repeated once and cells were resuspended in PBS 0.1% BSA 0.1% azide for FACS staining on ice (acid-treated samples).

All samples were counterstained with B220-FITC and analyzed by gating on $B220^+$ cells and measuring the (geometric) mean PE fluorescence of the population. Because endocytosis does not occur at 4°C, the level of PE fluorescence at 4°C with acid treatment was defined as the minimal fluorescence (Fmin). Maximal fluorescence (Fmax) was defined as the PE fluorescence at 4°C without acid treatment, which represents the starting amount of HEL-PE bound to the cells without endocytosis. Means of PE fluorescence obtained at 37°C with acid treatment provide the measure (F) of endocytosed PE in each condition or time point. To calculate the percent of initially bound HEL-PE that was endocytosed at each condition or time point, the formula (F-Fmin)/(Fmax-Fmin)×100 was used.

Recycling assay. HEL-SS-biotin was prepared from sulfo-NHS-SS-biotin (catalog no. 21331; Pierce Chemical Co.) according to the manufacturer's instructions. In brief, 1 ml HEL at 10 mg/ml in PBS was incubated with 166 μl sulfo-NHS-SS-biotin at 50 mM in PBS for 2 h on ice (molar excess of biotin to protein is 12). Reaction product was dialyzed in PBS to remove unreacted sulfo-NHS-SS biotin. Purified B cells were incubated with 10 μg/ml HEL-SS-biotin in medium for 30 min on ice. Cells were washed once with medium and incubated at 37°C for 10 min for endocytosis to occur. Endocytosis was then stopped by washing the cells with ice-cold medium, and surface biotin was cleaved by a 60-min treatment with medium without serum containing 50 mM 2-mercaptoethanesulfonic acid (MESNA; Sigma-Aldrich) on ice (22). Cells were washed with ice-cold medium and incubated for the indicated time at 37°C to allow reexpression of the receptors to the surface. Cells were washed in ice-cold PBS 0.1% azide and fixed in PBS 2% PFA for 20 min on ice. Finally, cells were stained with B220-FITC and SAV-PE in PBS 0.1% BSA 0.1% azide before FACS acquisition. Percentage of reexpressed receptor bound to antigen was calculated using the formula (F-Fmin)/(Fmax-Fmin)×100. F is the fluorescence obtained with SAV-APC for each condition. Fmin is the minimal fluorescence obtained for samples incubated for 10 min at 37°C, treated with MESNA for 1 h at 4°C, and not put back at 37°C for reexpression (MESNA, 0 min, 37°C).

Fmax is the maximal fluorescence obtained for samples incubated for 10 min at 4°C, left untreated for 1 h, and not put back at 37°C (no MESNA, 0 min, 4°C).

Filipin staining. This protocol is adapted from Muller et al. (21). Splenocytes were fixed in 3.2% PFA in PBS and stained for B220. Cells were then resuspended in PBS containing 30 μg/ml filipin, held at room temperature for 2 h, and directly analyzed on an LSR flow cytometer (Becton Dickinson).

Online supplemental material. Figs. S1–S6 show a series and additional images of cells from confocal fluorescence microscopy, and a schematic explaining the methods used for flow cytometric measurement of endocytosis and recycling. Figs. S1–S6 are available at http://www.jem.org/cgi/content/full/jem.20060552/DC1.

We thank the staff of the Medical Genome Centre for expert breeding and care of the mice and the staff of the JCSMR cytometry and imagery facilities for their help. We also thank Adrian Liston, Dr. Steve Martin, and Dr. Carola Garcia de Vinuesa for helpful discussions as well as Dr. Hai-Tao HE (CIML, France).

This work was supported by a fellowship from the Human Frontiers Science Program to M. Bléry and grants from the National Health and Medical Research Council.

The authors have no conflicting financial interests.

Submitted: 10 March 2006
Accepted: 25 May 2006

REFERENCES

1. Healy, J.I., R.E. Dolmetsch, L.A. Timmerman, J.G. Cyster, M.L. Thomas, G.R. Crabtree, R.S. Lewis, and C.C. Goodnow. 1997. Different nuclear signals are activated by the B cell receptor during positive versus negative signaling. *Immunity*. 6:419–428.
2. Dolmetsch, R.E., R.S. Lewis, C.C. Goodnow, and J.I. Healy. 1997. Differential activation of transcription factors induced by Ca2+ response amplitude and duration. *Nature*. 386:855–858.
3. Glynne, R., S. Akkaraju, J.I. Healy, J. Rayner, C.C. Goodnow, and D.H. Mack. 2000. How self-tolerance and the immunosuppressive drug FK506 prevent B-cell mitogenesis. *Nature*. 403:672–676.
4. Rui, L., C.G. Vinuesa, J. Blasioli, and C.C. Goodnow. 2003. Resistance to CpG DNA-induced autoimmunity through tolerogenic B cell antigen receptor-ERK signaling. *Nat. Immunol.* 4:594–600.
5. Benschop, R.J., K. Aviszus, X. Zhang, T. Manser, J.C. Cambier, and L.J. Wysocki. 2001. Activation and anergy in bone marrow B cells of a novel immunoglobulin transgenic mouse that is both hapten specific and autoreactive. *Immunity*. 14:33–43.
6. Wong, S.C., W.K. Chew, J.E. Tan, A.J. Melendez, F. Francis, and K.P. Lam. 2002. Peritoneal CD5+ B-1 cells have signaling properties similar to tolerant B cells. *J. Biol. Chem.* 277:30707–30715.
7. Weintraub, B.C., J.E. Jun, A.C. Bishop, K.M. Shokat, M.L. Thomas, and C.C. Goodnow. 2000. Entry of B cell receptor into signaling domains is inhibited in tolerant B cells. *J. Exp. Med.* 191:1443–1448.
8. Vilen, B.J., T. Nakamura, and J.C. Cambier. 1999. Antigen-stimulated dissociation of BCR mIg from Ig-alpha/Ig-beta: implications for receptor desensitization. *Immunity*. 10:239–248.
9. Vilen, B.J., K.M. Burke, M. Sleater, and J.C. Cambier. 2002. Transmodulation of BCR signaling by transduction-incompetent antigen receptors: implications for impaired signaling in anergic B cells. *J. Immunol.* 168:4344–4351.
10. Reth, M. 2001. Oligomeric antigen receptors: a new view on signaling for the selection of lymphocytes. *Trends Immunol.* 22:356–360.
11. Simons, K., and E. Ikonen. 1997. Functional rafts in cell membranes. *Nature*. 387:569–572.
12. Langlet, C., A.M. Bernard, P. Drevot, and H.T. He. 2000. Membrane rafts and signaling by the multichain immune recognition receptors. *Curr. Opin. Immunol.* 12:250–255.
13. Pierce, S.K. 2002. Lipid rafts and B-cell activation. *Nat. Rev. Immunol.* 2:96–105.
14. Rolli, V., M. Gallwitz, T. Wossning, A. Flemming, W.W. Schamel, C. Zurn, and M. Reth. 2002. Amplification of B cell antigen receptor signaling by a Syk/ITAM positive feedback loop. *Mol. Cell.* 10:1057–1069.
15. Reth, M. 2002. Hydrogen peroxide as second messenger in lymphocyte activation. *Nat. Immunol.* 3:1129–1134.
16. Cornall, R.J., J.G. Cyster, M.L. Hibbs, A.R. Dunn, K.L. Otipoby, E.A. Clark, and C.C. Goodnow. 1998. Polygenic autoimmune traits: Lyn, CD22, and SHP-1 are limiting elements of a biochemical pathway regulating BCR signaling and selection. *Immunity*. 8:497–508.
17. Chan, V.W., C.A. Lowell, and A.L. DeFranco. 1998. Defective negative regulation of antigen receptor signaling in Lyn-deficient B lymphocytes. *Curr. Biol.* 8:545–553.
18. Bell, S.E., and C.C. Goodnow. 1994. A selective defect in IgM antigen receptor synthesis and transport causes loss of cell surface IgM expression on tolerant B lymphocytes. *EMBO J.* 13:816–826.
19. Brink, R., C.C. Goodnow, J. Crosbie, E. Adams, J. Eris, D.Y. Mason, S.B. Hartley, and A. Basten. 1992. Immunoglobulin M and D antigen receptors are both capable of mediating B lymphocyte activation, deletion, or anergy after interaction with specific antigen. *J. Exp. Med.* 176:991–1005.
20. Christian, A.E., M.P. Haynes, M.C. Phillips, and G.H. Rothblat. 1997. Use of cyclodextrins for manipulating cellular cholesterol content. *J. Lipid Res.* 38:2264–2272.
21. Muller, C.P., D.A. Stephany, D.F. Winkler, J.M. Hoeg, S.J. Demosky Jr., and J.R. Wunderlich. 1984. Filipin as a flow microfluorometry probe for cellular cholesterol. *Cytometry*. 5:42–54.
22. Liu, H., M. Rhodes, D.L. Wiest, and D.A. Vignali. 2000. On the dynamics of TCR:CD3 complex cell surface expression and downmodulation. *Immunity*. 13:665–675.
23. Gschwendt, M., H.J. Muller, K. Kielbassa, R. Zang, W. Kittstein, G. Rincke, and F. Marks. 1994. Rottlerin, a novel protein kinase inhibitor. *Biochem. Biophys. Res. Commun.* 199:93–98.
24. Stoddart, A., M.L. Dykstra, B.K. Brown, W. Song, S.K. Pierce, and F.M. Brodsky. 2002. Lipid rafts unite signaling cascades with clathrin to regulate BCR internalization. *Immunity*. 17:451–462.
25. Stoddart, A., A.P. Jackson, and F.M. Brodsky. 2005. Plasticity of B cell receptor internalization upon conditional depletion of clathrin. *Mol. Biol. Cell.* 16:2339–2348.
26. Sproul, T.W., S. Malapati, J. Kim, and S.K. Pierce. 2000. Cutting edge: B cell antigen receptor signaling occurs outside lipid rafts in immature B cells. *J. Immunol.* 165:6020–6023.
27. Awasthi-Kalia, M., P.P. Schnetkamp, and J.P. Deans. 2001. Differential effects of filipin and methyl-beta-cyclodextrin on B cell receptor signaling. *Biochem. Biophys. Res. Commun.* 287:77–82.
28. Yamada, H., C.H. June, F. Finkelman, M. Brunswick, M.S. Ring, A. Lees, and J.J. Mond. 1993. Persistent calcium elevation correlates with the induction of surface immunoglobulin-mediated B cell DNA synthesis. *J. Exp. Med.* 177:1613–1621.
29. Dempsey, P.W., M.E. Allison, S. Akkaraju, C.C. Goodnow, and D.T. Fearon. 1996. C3d of complement as a molecular adjuvant: bridging innate and acquired immunity. *Science*. 271:348–350.
30. Cherukuri, A., P.C. Cheng, and S.K. Pierce. 2001. The role of the CD19/CD21 complex in B cell processing and presentation of complement-tagged antigens. *J. Immunol.* 167:163–172.
31. Batista, F.D., D. Iber, and M.S. Neuberger. 2001. B cells acquire antigen from target cells after synapse formation. *Nature*. 411:489–494.
32. Dintzis, H.M., R.Z. Dintzis, and B. Vogelstein. 1976. Molecular determinants of immunogenicity: the immunon model of immune response. *Proc. Natl. Acad. Sci. USA*. 73:3671–3675.
33. Dintzis, H.M., and R.Z. Dintzis. 1990. Antigens as immunoregulators. *Immunol. Rev.* 115:243–250.
34. Jun, J.E., L.E. Wilson, C.G. Vinuesa, S. Lesage, M. Blery, L. Miosge, M.C. Cook, E.M. Kucharska, H. Hara, J.M. Penninger, et al. 2003. Identifying the MAGUK-protein Carma-1 as a central regulator of humoral immune responses and atopy by genome wide mouse mutagenesis. *Immunity*. 18:751–762.
35. Sommer, K., B. Guo, J.L. Pomerantz, A.D. Bandaranayake, M.E. Moreno-Garcia, Y.L. Ovechkina, and D.J. Rawlings. 2005. Phosphorylation

of the CARMA1 linker controls NF-kappaB activation. *Immunity*. 23: 561–574.
36. Matsumoto, R., D. Wang, M. Blonska, H. Li, M. Kobayashi, B. Pappu, Y. Chen, and X. Lin. 2005. Phosphorylation of CARMA1 plays a critical role in T cell receptor-mediated NF-kappaB activation. *Immunity*. 23:575–585.
37. Shinohara, H., T. Yasuda, Y. Aiba, H. Sanjo, M. Hamadate, H. Watarai, H. Sakurai, and T. Kurosaki. 2005. PKC β regulates BCR-mediated IKK activation by facilitating the interaction between TAK1 and CARMA1. *J. Exp. Med.* 202:1423–1431.
38. Ceresa, B.P., and S.L. Schmid. 2000. Regulation of signal transduction by endocytosis. *Curr. Opin. Cell Biol.* 12:204–210.
39. Reichlin, A., A. Gazumyan, H. Nagaoka, K.H. Kirsch, M. Kraus, K. Rajewsky, and M.C. Nussenzweig. 2004. A B cell receptor with two Igα cytoplasmic domains supports development of mature but anergic B cells. *J. Exp. Med.* 199:855–865.
40. Mecklenbrauker, I., K. Saijo, N.Y. Zheng, M. Leitges, and A. Tarakhovsky. 2002. Protein kinase Cdelta controls self-antigen-induced B-cell tolerance. *Nature*. 416:860–865.
41. Goodnow, C.C., J. Crosbie, S. Adelstein, T.B. Lavoie, S.J. Smith-Gill, R.A. Brink, H. Pritchard-Briscoe, J.S. Wotherspoon, R.H. Loblay, K. Raphael, et al. 1988. Altered immunoglobulin expression and functional silencing of self-reactive B lymphocytes in transgenic mice. *Nature*. 334:676–682.